Color Vision Improvement of Anomalous Trichromats Based on a Wide-Color-Gamut Display

Jiafei Ma, Guan Wang, Cong Wang, Binghui Yao, Linxiao Deng, Chun Gu, and Lixin Xu

***Abstract*—Compared with normal color vision observers (NOs), anomalous trichromats (AT) have anomalous color vision responses owing to differences in cone sensitivity. The wide-color-gamut display provides a promising solution to this problem. Herein, we propose a color discrimination experiment based on a wide-color-gamut display. The observers' abilities to discern colors in various color directions were tested. The experimental findings were confirmed by simulations based on the shifting of the photopigments spectral absorption. It is concluded that the wide-color-gamut display significantly improves the color perception ability of AT, while proper light source optimization significantly enhances the visualization of AT. The study findings show that this AT-based, color vision model, may open up opportunities for future visual perception and biomedical applications.**

***Index Terms*—Anomalous trichromats, color discrimination, color gamut volume, laser display.**

I. Introduction

HUMAN color vision is based on the response of three cone photoreceptors located in the retina: L-, M-, and S-cone cells. Millions of cone cells are closely packed in the retina. They can be classified as long-, middle-, and short-wavelength-sensitive (L, M, and S) according to the peak positions of their relative sensitivities. The human eye perception of colors is the comprehensive result of the effects of different light radiations on the three visual pigments. Understanding the spectral sensitivity of long-wavelength sensitive (L-), medium-wavelength sensitive (M-), and short-wavelength sensitive (S-) wavelength-sensitive cone types is essential for the modeling of human color vision and the practical application of color matching and color specification. The derivation of cone fundamentals from psycho-physical data has been based on the work of Vos and Walraven [1], Smith and Pokorny [2], Stockman, Macleond and Johnson [3], and finally on Stockman, Sharpe and Fach [4] and Stockman and Sharpe [5].

Manuscript received March 27, 2022; accepted April 11, 2022. Date of publication April 14, 2022; date of current version May 6, 2022. This work was supported by the National Key Research and Development Program of China under Grant 2021YFF0307804. *(Corresponding author: Lixin Xu.)*

The authors are with the State Key Laboratory of Particle Detection and El-ectronics, University of Science and Technology of China, Hefei 230026, China (e-mail: majiafei@mail.ustc.edu.cn; wang1122@ustc.edu.cn; wonionw@mail.ustc.edu.cn; ybh1997@mail.ustc.edu.cn; dlx2988@mail.ustc.edu.cn; guchun@ustc.edu.cn; xulixin@ustc.edu.cn).

This work involved human subjects or animals in its research. Approval of all ethical and experimental procedures and protocols was granted by University of Science and Technology of China Hospital Ethics Committee.

Digital Object Identifier 10.1109/JPHOT.2022.3167444

People with color vision deficiency have abnormal cone cells, which arise from alterations in the gene encoding opsin molecules [6]. This leads to defects in the three-dimensional color vision of the anomalous trichromats (AT). According to the spectral shift of either the L-photopigment or the M-photopigment, AT is classified into several classes. The AT's L- or M-photopigment is identical with the exception of 15 of their 364 amino acids. The absorption maxima deviated by 31 nm [7]. The absorption spectrum of the M-photopigment can be converted completely to that of the L-photopigment only if the amino acids at positions 116, 180, 230, 233, 277, 285, and 309 are changed to those found in the L-photopigment. If any of the above positions of amino acids on two visual proteins in the cone cells is changed, a spectral shift related to normal cone cells will occur, which results in the approach between L and M sensitivity curves.

A lot of work has been done to simulate the color vision of AT, including experimental verification. Machado proposed AT can vary from mild to severe depending the amount of shift found in the peak sensitivity of the phtopigments [8]. Linhares found that even small changes in optical density and maximum sensitivity spectral position affect the display color gamut of anomalous observers when the method of visual cell-sensitive curve offset was used [9]. Simulations of anomalous color vision were calculated by fixating the optical density of the M and L cones and varying their spectral position or by fixating the anomalous spectral shift and by independently varying the M or L cones optical density. The display color gamut was estimated and its area in CIE 1976 UCS. Perales analyzed the effects of different light sources on the color discrimination ability of people by comparing their Rösch–MacAdam color volume [10]. The DeMarco *et al.* [11] data for spectral sensitivities were used to represent average AT. His theory is based on the assumption for the protanomalous a separation between the M and L' cone pigments of 10 nm and for the deuteranomalous a separation between the M' and L cone pigments of 6 nm. Yaguchi *et al.* proposed a multispectral imaging method to simulate the color appearance of AT [12]. He assumed that AT possess a protanomalous (green shifted) or deuteranomalous (red shifted) pigment instead of a normal (L or M) one. Luminance and two opponent color channels are converted into XYZ tristimulus values and then transformed into sRGB to reproduce a final image of AT. In the experiment, he tested the discrimination threshold of wavenumber shift of nine observers for simulation images of a deuteranope and a protanope. Traditionally, the different types of color defects are characterized by the Rayleigh

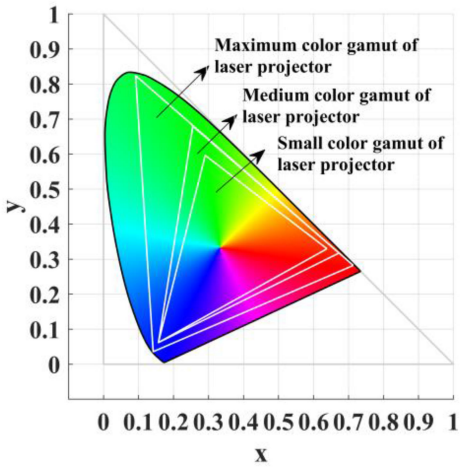

Fig. 1. Comparison of three color gamuts of the laser projector in CIE XYZ chromaticity diagram.

color matching, where the observer matches a spectral yellow to a mixture of spectral red and green. There may be specific limitations of the Rayleigh matching range as a measure of color discrimination [13].

Previous studies have focused on calculating the color gamut volume of the light source specified by CIE, or optimizing the spectrum to increase the AT's color gamut volume, or using Rayleigh matching to process the AT-perceived image. There is little research on the perception of AT in display scenarios. There is also no related work showing the color improvement of AT in a wide-color-gamut system. In the display system, the influence of brightness cannot be ignored. Compared with the flat color gamut, the three-dimensional color gamut based on a more uniform color space can describe the impact of brightness on the color gamut. It is critical to know which parts of the AT color gamut are missing or abnormal in the display. The light source of the laser display can be switched, and the color of these defects can be enhanced in a targeted manner, which is our purpose.

In this paper, we propose and demonstrate a method for measuring color gamut volume. Based on color discrimination experiments, it was proved that the wide-color-gamut display significantly improved the color perception ability of AT. Moreover, an efficient and fast algorithm was proposed to calculate the color gamut volume of AT in a display. The color gamut volume of AT can be optimized by changing the wavelength and spectral width of the light source.

II. Design of Color Discrimination Experiment

Thornton hypothesized that a high-color-discrimination light source can enhance the color discrimination ability of people with color vision deficits [14]. Based on the minimum perception threshold experiment, the color discrimination ability of observers in all color directions was obtained by discriminating a series of colors. Three color gamuts of display devices were selected for the experiments. Fig. 1 shows a comparison of three color gamuts of the laser projector on the CIE XYZ chromaticity diagram. For comparison, a color discrimination experiment was conducted for AT and NOs with the laser projector. Subsequently, the volume of the CIELAB color space and the number of discernible colors were calculated and used for the estimation of color diversity [15].

TABLE I
Three Color Gamuts of Laser Projector in the Color Discrimination Experiment

CIE XYZ	Small color gamut	Medium color gamut	Maximum color gamut
Color coordinates	R (0.6384, 0.3297) G (0.2904, 0.5964) B (0.1568, 0.0620) W (0.3147, 0.3335)	R (0.6727, 0.3174) G (0.2550, 0.6796) B (0.1568, 0.0618) W (0.3163, 0.3563)	R (0.7154, 0.2811) G (0.0949, 0.8220) B (0.1474, 0.0281) W (0.3133, 0.3382)
White luminance	188.3 cd/m^2	193.5 cd/m^2	196 cd/m^2

A. Experimental Setup

In the experiment, the projector was a laser projector manufactured by Barco and the model is 20C. For convenience, the color gamut of the projector is named as the small, medium, and maximum color gamut of the laser projector. These color gamuts were determined by adjusting the power ratio of each primary through the control panel of the projector. Table I shows the color coordinates of the three primary colors R, G, and B, and the white point W on the CIE XYZ chromaticity diagram, where the color coordinates were measured with a Konica CS2000 colorimeter. Before starting the experiment, the RGB coordinates of the color gamut of the projector were calibrated by changing the coordinates of the control panel, and calibrating with the actual measurement values of the colorimeter until the difference between the two is less than $\pm$ 0.002. The luminance of the laser display was adjusted 200 $\pm$ 20 cd/m^2 to ensure that the pattern could be observed in bright vision. The luminance of the three color gamuts are listed in Table I. In these luminance conditions, the response of the rod cells in the human eye is suppressed, and the response of the cone cells becomes dominant [16]. Experiments were performed in the three color gamuts to obtain the number of discernible colors in each gamut.

The psychological perception attributes of human eye color stimulation can be divided into lightness, chroma and hue angle. Based on this, the following color block experiment was designed. The specific experimental device is shown in Fig. 2. Nine color patches of the same size and hue were generated using an algorithm developed in MATLAB (version R2019b, MathWorks, Natick, MA, USA). The only difference is that one of the color patches was slightly more saturated compared with the other eight patches. The observers sat at 9.35 m in front of the laser projecting screen. This distance met the requirements of a 2-degree field-of-view (FOV) of the color block and a 10-degree FOV of the entire color discrimination page. Nine male observers (three deutans, four protans and two normal trichromats) aged 24–29 years participated in the experiment.

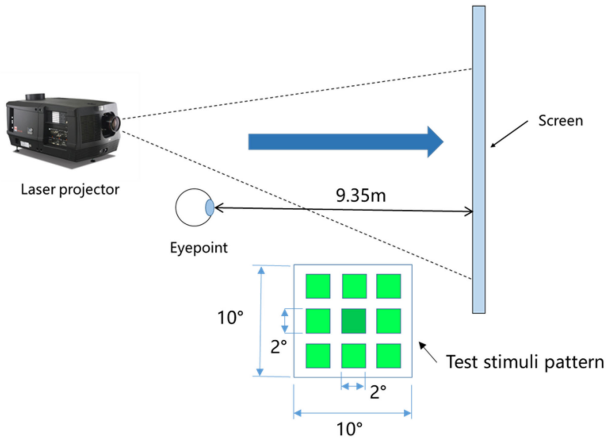

Fig. 2. Color discrimination experimental device and color stimulus.

AT were tested by Ishihara, and color weakness certificates were issued by the hospital of University of Science and Technology of China. All nine observers signed the informed consent form for the experiment. Before starting the experiment, the machine was adjusted and warmed up for two hours, then the observers perform a two-minute dark adaptation process. After reopening the test pattern, the observer performed a light adaptation for one minute. The experiments were conducted in a dark room, and the observers' task was to find a color block with higher chroma among the nine objects on the screen, and then use the numeric keyboard on their hands to select the number at the corresponding position. For each test, the observer initially obtained five scores. According to his/her answer,

1) If the judgment was correct, two points were added
2) If the judgment was false, four points were deducted

When the score increased to eight, the color discrimination was considered successful, and the chroma difference between the color blocks was reduced until the observers could not distinguish the difference. When the score dropped to zero, the color discrimination failed, and the chroma difference between the color blocks increased until the observer was able to perceive the difference. Thus, the color discrimination threshold at this chroma level could be determined. The chroma increased, the participants must perform a hue angle until the overall chroma became larger than 100. A concept needs to be clarified first that the overall chroma of the color block is, for example, 30, and a threshold experiment is performed at this chroma level. Combined with the advantages of staircase method [17], our experiment will have multiple judgments for each color stimulus pair, and get the stimulus pair closest to the threshold as much as possible. For each discrimination, regardless of whether the discrimination is successful or unsuccessful, the chroma step length of the next stimulus is maintained at minimum 0.5 units. Similar to the staircase method, in other words, observers need to distinguish the color block pairs that change by 0.5 chroma units each time, and respond to every test, with chroma adjusting accordingly, which greatly eliminates accidental errors.

In the color space, the chroma of the color is defined as:

$$C^*_{ab} = \left(\mathrm{a}^{*2} + \mathrm{b}^{*2}\right)^{\frac{1}{2}} \tag{1}$$

TABLE II
COMPARISON OF COLOR GAMUT AREAS MEASURED BY NINE OBSERVERS

Test subject	Small color gamut	Medium color gamut	Maximum color gamut
NO 1	1719.5	1801	2292.75
NO 2	940.5	1239.5	1450
AT 1	460.25	598.25	978.25
AT 2	206	350.75	419.5
AT 3	395	490	592
AT 4	440	456.5	578.5
AT 5	472.5	508.25	722.75
AT 6	223.75	274.5	298
AT 7	430.25	546.25	714

and the hue angle of the color is defined as:

$$h_{ab} = \arctan\left(b^*/a^*\right) \tag{2}$$

The hue angle ranged from 0° to 360°. Twelve color directions were selected at equal intervals in the program as follows: 0, 30, 60, 90, 120, 150, 180, 210, 240, 270, 300, and 330. After the overall saturation level of one hue angle reaches 100, the program will switch to the next hue angle in order to repeat the experiment until all 12 hue angles are completed. Finally, the program will give 12 columns of chroma data. The number of colors distinguished by the observer was measured in each color direction based on the minimum perceptible difference [18]. The participants had to distinguish colors at all 12 hue angles in three color gamuts. Therefore, the number of distinguished colors under 12 hue angles is obtained.

B. Experimental Results and Analysis

A comparison of the three color gamuts of the laser projector based on the CIEXYZ chromaticity diagram is shown in Fig. 1. The number of distinguished colors of the observer at each hue angle is connected with a line, which can approximate the observer's color gamut, which are shown in Fig. 3. It was found that a laser projection system with a wider color gamut can improve the observers' visual experience; in particular, the color gamut of AT under almost all hue angles improved. For a single observer, a wider color gamut display can expand the color gamut he sees, which can improve his viewing experience. Among the two NOs, the numbers of colors discerned for 12 hue angles measured experimentally were also quite different because the response curves of the three types of cone cells in different people were not the same. Similarly, compared with normal observers, the curves of cone cells of observers with color weaknesses were shifted, which resulted in a deviation of color perception. Since the spectral separation between the two cones is reduced, in order to obtain the same color difference signal, an approximately exponentially large color difference is required. In the case of the same saturation range, the number of distinguishable colors of AT is less than that of NOs. The color gamuts of AT were much smaller than those of the normal observers.

Table II lists the color gamut areas obtained by the nine observers in the color discrimination experiments in the cases of three color gamuts. It can be noted that with an increase in the color gamut, the color gamut area of AT also increased,

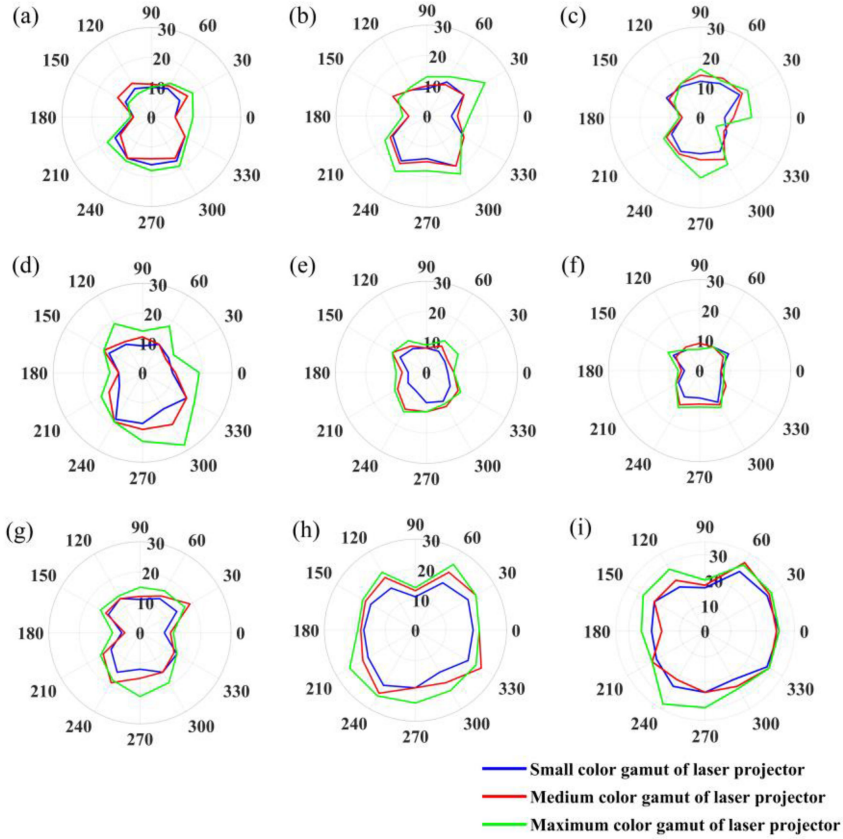

Fig. 3. Schematic of the color discrimination abilities of the two NOs and seven AT for 12 hue angles. (a), (b), (c) Observer 1, 2 and 3 are deutans. (d), (e), (f), (g) Observer 4, 5, 6 and 7 are protans. (h, i) Normal observers 1 and 2. The areas enclosed by lines of different colors represent the color gamut of the observer at the different color gamut of the projector. The radial numbers in the figure indicate the number of colors distinguished by the observer in the range of chroma 0–100, while the angle numbers in the figure indicate different hue angles. The experiment was based on $L^* = 50$ planes in the CIELAB color space.

and the increase was larger than that of normal observers. For all nine observers, increasing the color gamut of the projector can increase the color gamut area. It should be noted that these results only represent the number of distinguished colors of each observer at different hue angles. They are relative sizes and cannot be used as absolute measures. However, in the relatively uniform CIELAB color space, the number of distinguishable colors should be considered proportional to the distance from the color gamut boundary to the center.

III. Simulation of AT

Compared with the early CRT displays and Xenon lamp projectors to today's laser display, the wide-color-gamut display with laser can improve people's color perception. Moreover, there is no research to simulate the color gamut of AT under different display color gamut. Based on the above experimental results, a method was proposed to calculate the color gamut volume of AT. By analyzing the color gamut volume of AT, the color gamut can be optimized by changing some parameters.

Fig. 4 shows the 2-degree LMS fundamentals of normal trichromats based on the Stiles and Burch [19] 10-degree CMFs (color matching functions) adjusted to 2-degree. The peaks of M- and L-cone are 27.4 nm apart on the wavelength axis. According

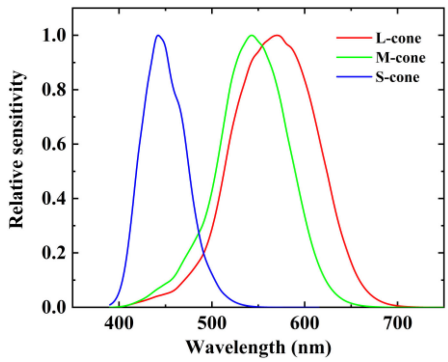

Fig. 4. L-, M-, and S-cone fundamentals for normal observers by Stockman [5].

to Asenjo *et al.* [7], amino acid residues at positions 116, 180, 230, 233, 277, 285, and 309 can determine the spectral properties of opsin. About a 30 nm difference in wavelength of the maximum absorption of the L- and M-photopigments is thought to be caused by these seven amino acid residues. Baylor *et al.* [17] and Lamb [20] showed that photopigments have an identical shape on a log wavenumber abscissa. We adopted the hypothesis of Hirohisa [12] that the spectral quantal absorption of the L- and

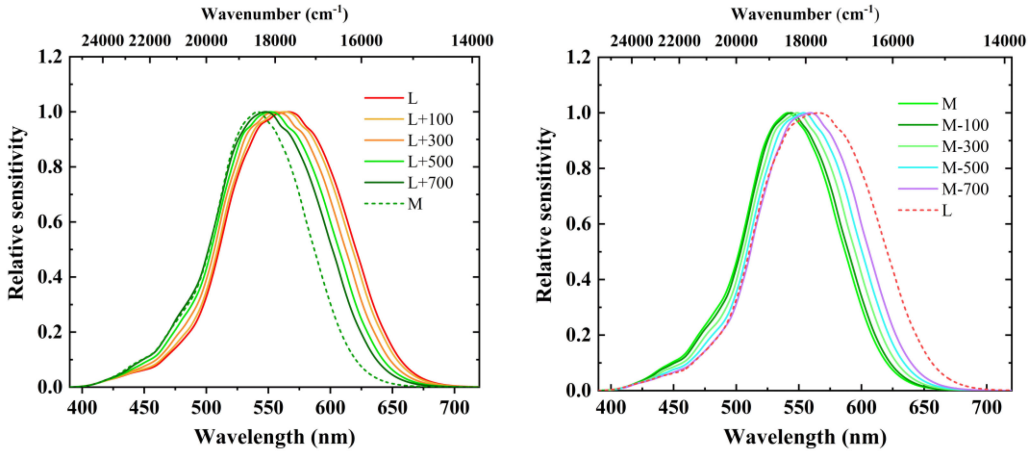

Fig. 5. Simulations of cone fundamentals for (a) protanomalous and (b) deuteranomalous observers.

M-phtopigments should shift along the wavenumber from the normal spectral absorption, which is expressed as (3) and (4):

$$\begin{aligned} \log A_L^{'}(\nu) &= \log A_L(\nu - \Delta\nu) \\ \log A_M^{'}(\nu) &= \log A_M(\nu + \Delta\nu) \end{aligned} \tag{3}$$

$A'_L(\nu)$ and $A_L(\nu)$ are L-photopigments absorptance spectral in terms of quanta of a normal trichromat and a protanomaly, respectively, and $A'_M(\nu)$ and $A_M(\nu)$ are the spectral absorption of the M-photopigments of a normal trichromat and a deuteranomaly, respectively. Considering the optical density of macular and ocular media, the fraction of the incident light at the retinal level absorbed in the cones, or the absorptance spectral in terms of quanta, is [21]:

$$\begin{aligned} a_{i,l}(\lambda) &= 1 - 10^{\left[-D_{\tau,max,l} \cdot A_{i,0(L-pigment)}(\lambda)\right]} \\ a_{i,m}(\lambda) &= 1 - 10^{\left[-D_{\tau,max,m} \cdot A_{i,0(M-pigment)}(\lambda)\right]} \\ a_{i,s}(\lambda) &= 1 - 10^{\left[-D_{\tau,max,s} \cdot A_{i,0(S-pigment)}(\lambda)\right]} \end{aligned} \tag{4}$$

$A_{i,0}(\lambda)$ is the low density spectral absorbance of the visual pigment. For L-cones, M-cones and S-cones, the peak densities $D_{\tau,max}$ are 0.5, 0.5 and 0.4 at a 2° field size, respectively. The cone fundamental sensitivity in terms of quanta is given by the cone absorptance spectral in terms of quanta multiplied by the tansmittance at every wavelength:

$$\begin{aligned} \bar{l}_q(\lambda) &= a_{i,l,2}(\lambda) \cdot \tau_{macula}(\lambda) \cdot \tau_{ocul}(\lambda) \\ \bar{m}_q(\lambda) &= a_{i,m,2}(\lambda) \cdot \tau_{macula}(\lambda) \cdot \tau_{ocul}(\lambda) \\ \bar{s}_q(\lambda) &= a_{i,s,2}(\lambda) \cdot \tau_{macula}(\lambda) \cdot \tau_{ocul}(\lambda) \end{aligned} \tag{5}$$

Similarly, we can use the above method to calculate AT cone fundamentals. By converting the 2° cone fundamentals $\bar{l}_q(\lambda)$, $\bar{m}_q(\lambda)$ and $\bar{s}_q(\lambda)$ in terms of quanta into 2° cone fundamentals $\bar{l}(\lambda)$, $\bar{m}(\lambda)$, and $\bar{s}(\lambda)$ in terms of energy one should multiply by λ and renormalize at the nearest 0.1 nm to the maximum values, respectively at 570.2 nm, 542.8 nm and 442.1 nm. Fig. 5 shows cone fundamentals derived by different offsets of peak values of L- and M-photopigments absorptance spectral in terms of energy on the wavenumber axis. The left figure shows the curves obtained by moving the peak of L-photopigments absorptance spectral by 100, 300, 500, 700 cm^{-1} along the wavenumber axis, respectively. The right figure shows the curves obtained by moving the peak of M-photopigments absorptance spectral in terms of energy by 100, 300, 500, 700 cm^{-1} along the wavenumber axis, respectively. Subsequently, the AT cone fundamentals were converted to X'Y'Z' stimulation values by applying Stockman's transformation [22].

Ou-Yang proposed a three-dimensional color volume boundary description of color displays, which can be precisely constructed from the two-dimensional polygon gamut area [23]. As the brightness increases, the color gamut area on the color coordinates shrinks, and the color gamut polygon area under different brightness is determined by the vertices. Masaoka [24] proposed the estimation of the CGV (color gamut volume) of display. The vertices of each polygon are determined by a combination of color channel values lying on the gamut surface. When the color channels are arranged in the hue direction, the values contain two types. On the basis of previous research, we proposed to calculate the CGV of AT in the tri-chromatic RGB display. The calculation of polygon is based on the xyY color space, where Y represents luminance. In order to standardize color accurately, 630, 532, 467 nm were selected as tri-chromatic RGB light source. The spectrum of the three primary colors was set to a Gaussian distribution with a spectral width of 1 nm. The range of wavelengths covers visible light from 390 nm to 830 nm. Both the color matching function and the light source must be interpolated so that the function has adequately small wavelength step, such as 0.1 nm, and the sampling wavelengths match each other. According to the recommendation of CIE [21], spline interpolation is used instead of linear interpolation for the light source spectrum, and linear interpolation is used for the color matching function. The total luminance Y_t can be calculated according to the X'Y'Z' stimulus values of AT and the spectral data of the three primary colors. To estimate CGV of AT in the display, polygon were calculated in two types

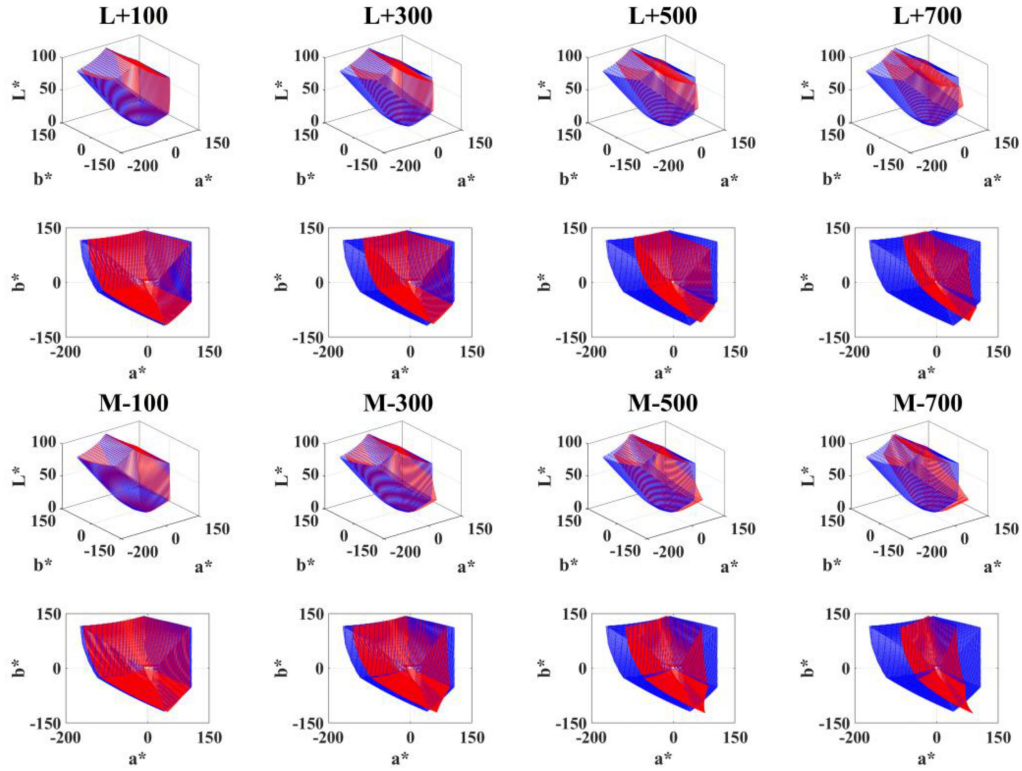

Fig. 6. Color gamut in CIELAB color space for protanomalous (green-shifted L-photopigments) and deuteranomalous (red-shifted M-photopigments). The blue part is the color gamut of normal observers as a control.

according to which zone Y_t belongs to. Interpolating 1000 points for each constant lightness plane, in this way, the 3-D contour of the gamut boundary under different luminance is obtained. These data were transformed into the CIELAB color space with the lightness ranged from 1 to 99 at intervals of 1 and the peak lightness of the white point normalized to 100.

A. Color Gamut Volume With Different Offsets

For easier comparison, the white point of the three primary color light sources was set to the coordinates of D65. Fig.6 shows CGV and the top view of CGV for protanomalous (green-shifted L-photopigments) and deuteranomalous (red-shifted M-photopigments). The blue area represents the color g-amut of the NOs, and the red area represents the color gamuts of AT at different offsets along the wavenumber axis. The results of CGV are consistent with that of Perales [25] in 2010. The color gamut of deuteranomal and protanomal are reduced to a certain extent relative to the color gamut of NOs. The number of discernible colors estimated of CGV for normal and color-deficient observers are listed in Table III, which were calculated by adding up the area of each layer of lightness from 1 to 99. The number of colors perceived by each class of observers is then estimated by the color volumes enclosed by color gamut boundary. For the CIELAB representation, the color volume for AT is smaller than the color volume for NOs. And the larger the offset, the smaller the color volume. Under the same offset, the color volume of protanomalous is slightly larger than that of deuteranomalous. In terms of color, the offset for photopigments along the wavenumber axis significantly reduced the red and green axis of the CIELAB color space. It is worth mentioning that the color solid of AT surpasses that of NOs. This shows that as the photopigment response curve shifts, AT perceive colors that NOs can't perceive. There are similar conclusions in Perales' paper [25].

TABLE III
NUMBER OF DISCERNIBLE COLORS ESTIMATED FOR THE COLOR SOLID FOR NORMAL AND COLOR-DEFICIENT OBSERVERS

Number of Discernible Colors (D65) CIELAB	
Normal	1880889
L+100	1730568 (92%)
L+300	1424818 (76%)
L+500	1176766 (63%)
L+700	915226 (49%)
M-100	1785779 (95%)
M-300	1582382 (84%)
M-500	1284031 (68%)
M-700	950413 (51%)

B. Effects of Peak Wavelength and Spectral Width of Primaries on Color Gamut Volume

The wavelengths of the three primary color light sources used to simulate the optimal color are 630 nm, 532 nm, and 467 nm, respectively. The spectral widths of the three primary color light sources were set to 1 nm, and the waveforms were all Gaussian.

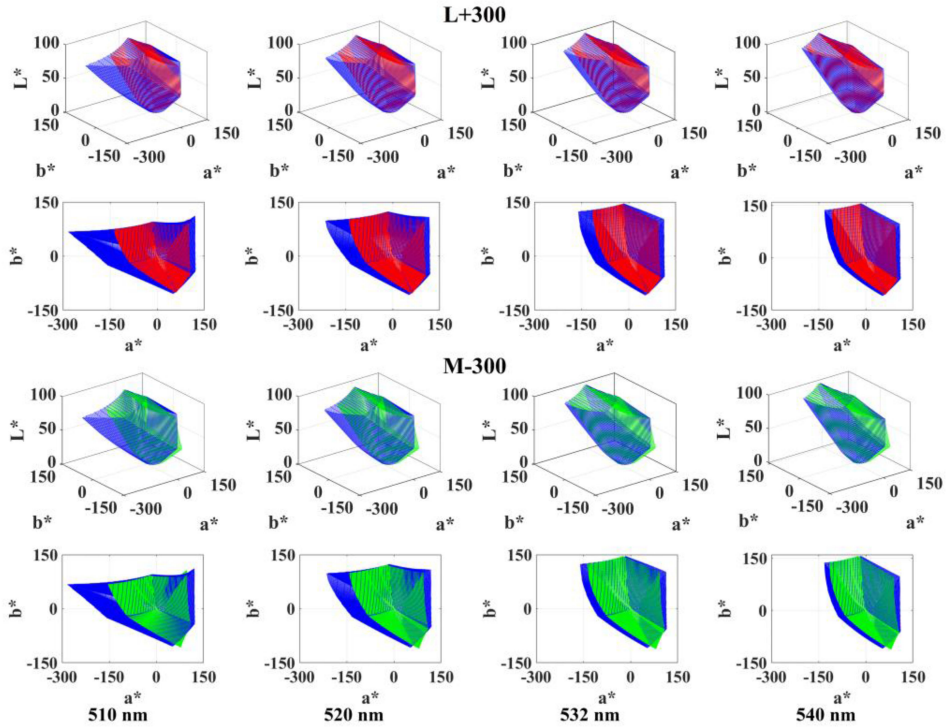

Fig. 7. Color gamut in CIELAB color space for protanomalous (L-photopigments green-shifts 300 cm^{-1}) and deuteranomalous (M-photopigments red-shifts 300 cm^{-1}) when the green wavelength are 510 nm, 520 nm, 532 nm, and 540 nm, respectively. The blue part is the color gamut of normal observers under the same conditions as a control.

However, the wavelength and spectral width of the light source obviously affect the color gamuts of the observers with normal color vision, including those with AT. Perales *et al.* studied the effects of three-band spectra with high-color-discrimination ability for normal observers on the color discrimination ability of people with color vision defects [10]. The light source optimized based on the spectrum can improve considerably the resolution of red–green anomalies, but it is almost neutral for dichromats. Therefore, the choice of red and green light sources is critical for the AT. Fig. 7 shows the CGV when L and M shifts 300 cm^{-1}, respectively, and the green wavelengths are 510 nm, 520 nm, 532 nm, and 540 nm. For better visualization of the differences between AT and NOs, two color areas are used to represent the color gamut of AT and NOs. The blue areas in each subgraph represent the color gamuts of NOs, and the red areas and green areas represent the color gamuts of AT. The main reduction for AT is found for red and green regions of the color space. But as the wavelength of green light increases, the yellow region of the color space is found to increase. Fig. 8 shows the CGV of L (green-shifts 300 cm^{-1}) and M (red-shifts 300 cm^{-1}) when the wavelength of red light are 630 nm, 650 nm, 670 nm, and 690 nm, respectively. The change in wavelength of the red light has no prominent effect on the color gamut of AT and NOs. Fig. 9 shows the color gamut volume trend when the wavelength or spectral width of the light source changes. For protanomals where the peak sensitivity of the L-cone shifts 300 cm^{-1}, the maximum value is obtained at 520 nm with the green wavelength increasing. For deuteranomaly where the peak sensitivity of the M-cone shifts 300 cm^{-1}, the maximum value is obtained at 532 nm with the green wavelength increasing. With the wavelength of the red light source increasing from 630 nm to 690 nm, the color gamut volume increased by only 6% for AT and NOs, but the increasement is not significant and tended to be saturated.

The spectral width of the green light source increased from 10 nm to 40 nm, and the color gamut volume decreased. This represents a 36% reduction in total, while the spectral width of the red light source increased from 10 nm to 40 nm, and the color gamut volume decreased by 17%. For the M shift of 300 cm^{-1}, the change in the spectral width of the green light source first increased and then decreased the color gamut volume, achieving a maximum value at the 30 nm width of the green spectrum. This shows that different types of AT responded differently to changes in the width of the green spectrum. The color gamut of the green light source decreased faster with an increase in the spectral width compared with the red light source. Therefore, the change in green has the greatest impact on the overall color gamut volume. However, when the spectral sensitivity curve of the cone cells is shifted, the increase in the spectral width of the light source does not necessarily lead to a decrease in the color gamut. Therefore, it is necessary to choose the appropriate light source for different types of AT.

C. Discussion

Based on the above data and the theory described above, the color gamut volume of NOs and AT on the $L* = 50$ planes was calculated, as shown in Fig. 10. Applying our theory to analyze

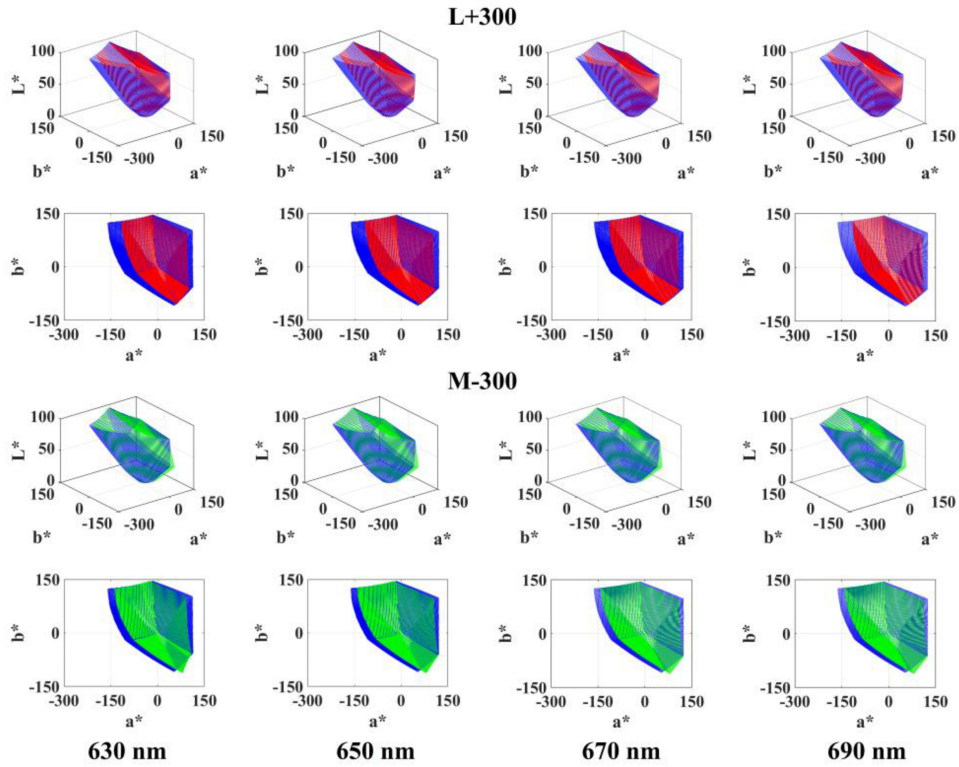

Fig. 8. Color gamut in CIELAB color space for protanomalous (L-photopigments green-shifts 300 cm^{-1}) and deuteranomalous (M-photopigments red-shifts 300 cm^{-1}) when the red wavelength are 630 nm, 650 nm, 670 nm, and 690 nm, respectively. The blue part is the color gamut of normal observers under the same conditions as a control.

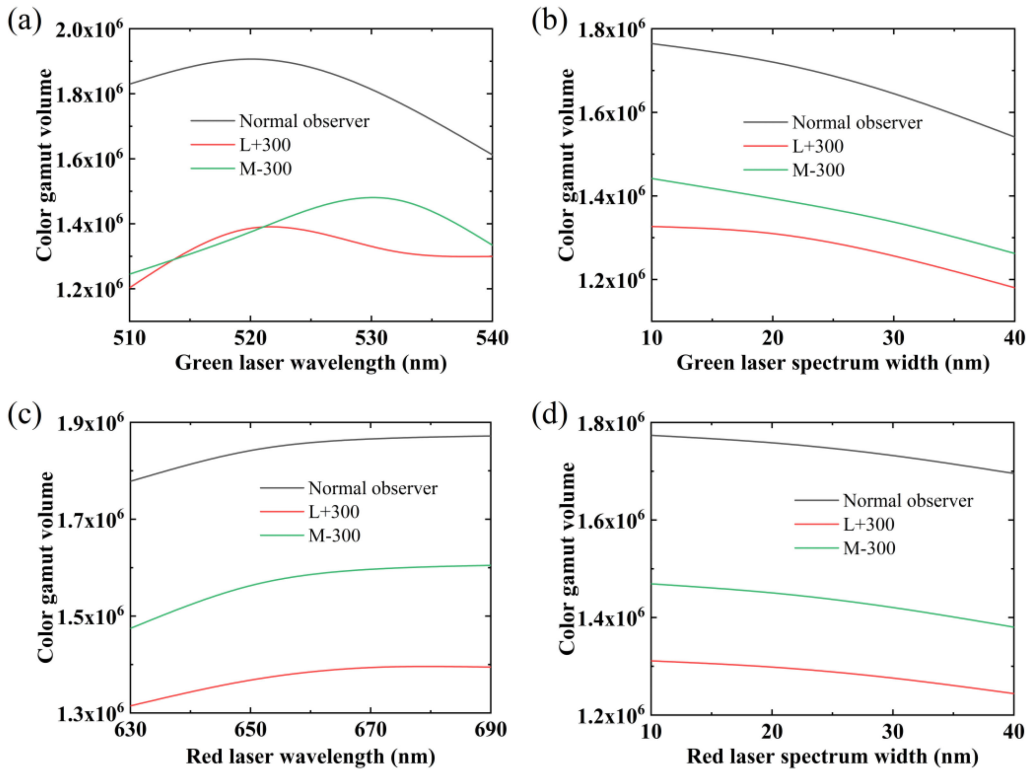

Fig. 9. Color gamut volume trend when the wavelength or spectral widths of the light source vary.

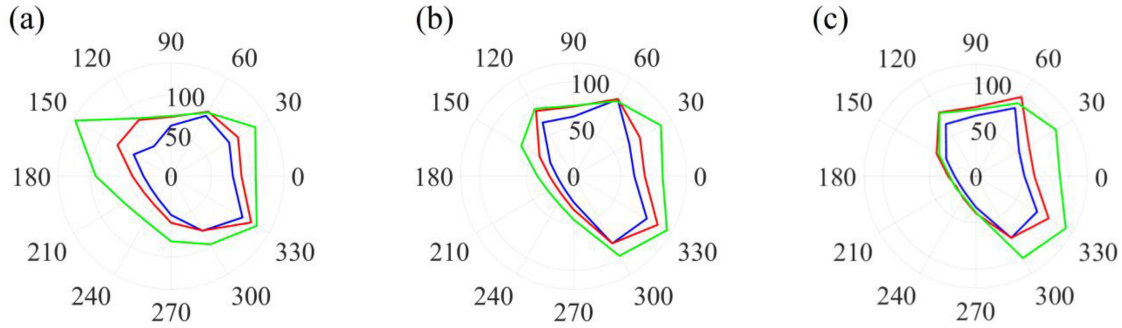

Fig. 10. (a) Normal observers. (b) Observers with defective color vision with L shifting by 300 cm^{-1}. (c) Observers with defective color vision with M shifting by 300 cm^{-1}. The green line indicates the color gamut of the observer with the projector the maximum color gamut. Similarly, the red line indicates the medium color gamut, and the blue line indicates the small color gamut.

the color gamut of AT and those with NOs, the $L* = 50$ planes in the CIELAB space were selected for comparison. The $L* = 50$ planes had the largest gamut area, which is convenient for intuitive comparisons [26]. We theoretically analyzed the color gamuts of NOs and AT with L- or M-cone shifting 300 cm^{-1} in the three color gamuts applied in the experiment. The theoretical calculations of the color gamut areas in Fig. 10(a) are equal to 12182, 17228, and 27224. For AT with L shifting 300 cm^{-1}, the $L* = 50$ plane color gamut area is 9943, 13045, and 17739, respectively. For AT with M shifting by 300 cm^{-1}, the $L* = 50$ plane color gamut areas is 8539, 11785, and 15989, respectively. As the color gamut used in the experiment increases, the color gamut of the observer shows an increasing trend. This indicates that a wide-color-gamut display has a significant effect on the color gamut of the human visual system. The color gamuts of AT with L or M shifting 300 cm^{-1} is significantly smaller than those of observers with normal color vision.

Fig. 3 shows that the color gamuts of observers are different even if the light source is the same. This shows a relatively large individual difference. The color gamut of AT is much smaller than that of the NOs on the $L* = 50$ planes. The same result can support our conclusion in other class of AT. Table IV shows the comparison between experimental data and theoretical data of the number of colors that the observers can distinguish. All values are relative values, and each small-color-gamut result is specified as 100%, and the results of the wider gamut are ratios of the small gamut results. Both experimental and theoretical simulation results show that wide-color-gamut enhances color perception in AT with different severity. It is worth noting that the wide-color-gamut enhancement results in theory are basically higher than that in experiment. This is mainly due to the existence of the human eye color discrimination ellipse. In theoretical analysis, our data comes from the average of big data samples, and there are differences with actual individuals. Just like the experimental data shown in Table II, there are also large differences among normal observers. This requires an accurate instrument that can quickly and accurately obtain the tristimulus value of the human eye, so that the calculation result will be faster and more accurate. However, in terms of theoretical analysis and experimental results, our theory is more consistent with the color perception of abnormal observers.

TABLE IV
COMPARISON BETWEEN EXPERIMENTAL DATA AND THEORETICAL DATA OF THE NUMBER OF COLORS THAT THE OBSERVER CAN DISTINGUISH

Test subject	Small color gamut	Medium color gamut	Maximum color gamut
Experimental results			
NO 1	100 %	104.5 %	133.3 %
NO 2	100 %	131.8 %	154.2 %
AT 1	100 %	130.0 %	212.5 %
AT 2	100 %	170.3 %	203.6 %
AT 3	100 %	124.0 %	150.0 %
AT 4	100 %	103.8 %	131.5 %
AT 5	100 %	107.6 %	153.0 %
AT 6	100 %	122.7 %	133.2 %
AT 7	100 %	127.0 %	166.0 %
Theoretical results			
NO	100 %	141.4 %	223.5 %
L+100	100 %	134.9 %	198.8 %
L+300	100 %	131.2 %	178.4 %
L+500	100 %	131.2 %	175.7 %
L+700	100 %	143.8 %	190.9 %
M-100	100 %	133.7 %	198.9 %
M-300	100 %	138.0 %	187.2 %
M-500	100 %	140.1 %	202.7 %
M-700	100 %	134.9 %	214.3 %

We experimentally and theoretically demonstrate the promise of the wide-color-gamut laser display in solving color vision defects of AT. Our experiments and theories have confirmed that the wide-color-gamut display technology makes it possible for AT to perceive more colors. Moreover, the theoretical study in Fig. 7 shows that the adjustment of the central wavelength of the green light source in the display system can increase the coverage of the color stereo between AT and normal trichromats. Our results point to strong compensation for color loss in AT through optimization of color gamut in the laser display. Our method not only has a similar effect on laser display, but also on other WCG displays, such as quantum dot display [27], whose color gamut can achieve over 97% Rec. 2020 standard. Osamu Masuda researched the lighting spectrum to maximize colorfulness [28]. The spectral profile of white illumination maximized the theoretical limit of perceivable object colors. This suggested that the color temperature of the white light source had a significant

influence on the color perceived by the AT. In the experiment, the color temperature of our light source was not consistent, which may have resulted in measurement errors. Accordingly, the light source requires more precise control. When the color gamut of the display device changes, the color gamut of the observer also changes accordingly. Therefore, the wavelength and spectral width of the light source are changed to increase the color gamut of the observers. Our theory and experiments provide a reference for the color discrimination of AT with wide color gamut.

Several approaches have been proposed to assist the people with color vision deficits in distinguishing colors. These approach include optical approach as well as recoloring methods. Optical approach use the notch filter [29], and the most famous production is EnChroma. The principle is to reduce the overlap between the spectra sensitivity functions of the L, M and S cone cells. The notch filter may unnecessarily filter away color that color vision deficiency can well distinguish even without the filter. Recoloring approach is mainly for displaying digital visual content. For example, the accessibility feature "color filters/ color correction" implemented in iOS/Android equipment. The color adjustment of these methods does not involve an increase in the number of colors, but a redistribution of colors in the image. In this paper, the laser display with wide-color-gamut increases the number of colors perceived by AT, and the characteristics of high-color-saturation improve the color resolution of AT. But better results require a combination of hardware and algorithms, for which our results provide a good reference. There are also some studies of neural adaptation. Werner analyzed the adaptive changes in color vision from long-term filter usage in AT [30]. After using the filter for a long time, the nervous system has an adaptability, and the response of AT is increased. Similarly, the wide-gamut-display is also likely to have adaptive enhancements to the nervous system of AT. In this way, it will be an interesting job whether the enhancement effect of the nervous system will be maintained during the period of not watching the display.

The results presented herein are obtained by expressing the color boundary in the CIELAB space, which is not an absolutely uniform color space. Because the experimental measurement here is a correlation estimate rather than an absolute value, these non-uniformities have minor effects on the inferences.

The proposed model is a color gamut model based on the LMS cone fundamentals of AT. We adopt the log-wavenumber-shifting model proposed by Yaguchi [12]. The LMS model proposed by Yaguchi takes into account the correction of the retinal macular pigment and the lens pigment, so that the generated AT stimulation value is more accurate and comprehensive. Different from the research of Yaguchi, our paper focus on the calculation of the stereo color gamut, because in a display system, brightness is a non-negligible quantity, and the color perceived by AT needs to be represented in the stereo color gamut. Combined with our proposed color discrimination experiments based on display systems, our theory can well predict how the AT perceives colors in a stereo color space. Only the average values of the LMS data published by Stockman were considered in this study [5]. However, there were individual differences in the LMS response curves of AT, which led to the differences in the relative values of the experimental results and theoretical analysis outcomes at different hue angles. Moreover, a large number of observers, especially AT, are needed to perform human eye color discrimination experiments so that the optimal solution can be found for the selection of the light source of the projection equipment.

IV. Conclusion

We proposed a method to measure the color gamut volumes of AT and NOs based on color discrimination experiments. The results proved that the color gamut of AT increased with the color gamut of display expanded. This indicates that the wide color gamut can improve considerably the color discrimination ability of AT. To simulate the color gamut volume of different types of AT, an offset method based on the spectral response curve of photopigments was proposed. This method is in good agreement with the experimental results, and the color gamut volume of AT can be increased by optimizing the wavelength and spectral width of the light source in the display device. This work can provide a reference for the selection and optimization of light sources for display devices for people with varying color vision capacities. This will be helpful in future displays and biomedical customized products.

References

[1] J. J. Vos and P. L. Walraven, "On the derivation of the foveal receptor primaries," *Vis. Res.*, vol. 11, pp. 799–818, 1971.
[2] V. C. Smith and J. Pokorny, "Spectral sensitivity of the foveal cone photopigments between 400 and 500 nm," *Vis. Res.*, vol. 15, pp. 161–171, 1975.
[3] A. Stockman, D. I. MacLeod, and N. E. Johnson, "Spectral sensitivities of the human cones," *J. Opt. Soc. Am. A. Opt. Image. Sci. Vis.*, vol. 10, pp. 2491–2521, 1993.
[4] A. Stockman, L. T. Sharpe, and C. Fach, "The spectral sensitivity of the human short-wavelength sensitive cones derived from thresholds and color matches," *Vis. Res.*, vol. 39, pp. 2901–2927, 1999.
[5] A. Stockman and L. T. Sharpe, "The spectral sensitivities of the middle- and long-wavelength-sensitive cones derived from measurements in observers of known genotype," *Vis. Res.*, vol. 40, pp. 1711–1737, 2000.
[6] S. L. Merbs and J. Nathans, "Absorption spectra of the hybrid pigments responsible for anomalous color vision," *Science*, vol. 258, pp. 464–466, 1992.
[7] A. B. Asenjo, J. Rim, and D. D. Oprian, "Molecular determinants of human red/green color discrimination," *Neuron*, vol. 12, pp. 1131–1138, 1994.
[8] G. M. Machado, M. M. Oliveira, and L. A. Fernandes, "A physiologically-based model for simulation of color vision deficiency," *IEEE. Trans. Vis. Comput. Graph.*, vol. 15, no. 6, pp. 1291–1298, Nov.–Dec. 2009.
[9] J. M. M. Linhares, J. L. A. Santos, V. M. N. de Almeida, C. A. R. João, and S. M. C. Nascimento, "The display gamut available to simulate colors perceived by anomalous trichromats," *Comput. Color Imaging2015*, vol. 9016, pp. 104–110, 2015.
[10] E. Perales, J. M. Linhares, O. Masuda, F. M. Martinez-Verdu, and S. M. Nascimento, "Effects of high-color-discrimination capability spectra on color-deficient vision," *J. Opt. Soc. Am. A. Opt. Image. Sci. Vis.*, vol. 30, pp. 1780–1786, 2013.
[11] P. DeMarco, J. Pokorny, and V. C. Smith, "Full-spectrum cone sensitivity functions for X-chromosome-linked anomalous trichromats," *J. Opt. Soc. Am. A.*, vol. 9, pp. 1465–1476, 1992.
[12] H. Yaguchi, J. Luo, M. Kato, and Y. Mizokami, "Computerized simulation of color appearance for anomalous trichromats using the multispectral image," *J. Opt. Soc. Am. A. Opt. Image. Sci. Vis.*, vol. 35, pp. B278–B286, 2018.
[13] J. Bosten, "The known unknowns of anomalous trichromacy," *Curr. Opin. Behav. Sci.*, vol. 30, pp. 228–237, 2019.
[14] W. A. Thornton, "Color-discrimination index," *J. Opt. Soc. Am.*, vol. 62, pp. 191–194, 1972.

[15] F. Martinez-Verdu, E. Perales, E. Chorro, D. de Fez, V. Viqueira, and E. Gilabert, "Computation and visualization of the macadam limits for any lightness, hue angle, and light source," *J. Opt. Soc. Am. A. Opt. Image. Sci. Vis.*, vol. 24, pp. 1501–1515, 2007.

[16] M. Aguilar and W. S. Stiles, "Saturation of the rod mechanism of the retina at high levels of stimulation," *Optica Acta: Int. J. Opt.*, vol. 1, pp. 59–65, 2010.

[17] D. A. Baylor, B. J. Nunn, and J. L. Schnapf, "Spectral sensitivity of cones of the monkey macaca fascicularis," *J. Physiol.*, vol. 390, pp. 145–160, 1987.

[18] R. H. Gracely, L. Lota, D. J. Walter, and R. Dubner, "A multiple random staircase method of psychophysical pain assessment," *Pain*, vol. 32, pp. 55–63, 1988.

[19] W. S. Stiles and J. M. Burch, "N.P.L. Colour-matching investigation: Final report (1958)," *Optica Acta: Int. J. Opt..*, vol. 6, pp. 1–26, 2010.

[20] T. D. Lamb, "Photoreceptor spectral sensitivities: Common shape in the long-wavelength region," *Vis. Res.*, vol. 35, pp. 3083–3091, 1995.

[21] CIE Publ. 170-1:2006, "Fundamental chromaticity diagram with physiological axes–part 1," *Vienna: CIE Central Bureau*, 2006, pp. 170–171.

[22] V. C. Smith and J. Pokorny, "Spectral sensitivity of color-blind observers and the cone photopigments," *Vis. Res.*, vol. 12, pp. 2059–2071, 1972.

[23] M. Ou-Yang and S. W. Huang, "Determination of gamut boundary description for multi-primary color displays," *Opt. Exp.*, vol. 15, pp. 13388–13403, 2007.

[24] K. Masaoka, F. Jiang, M. D. Fairchild, and R. L. Heckaman, "Analysis of color volume of multi-chromatic displays using gamut rings," *J. Soc. Inf. Display*, vol. 28, pp. 28273–28286, 2020.

[25] E. Perales, F. M. Martinez-Verdu, J. M. Linhares, and S. M. Nascimento, "Number of discernible colors for color-deficient observers estimated from the macadam limits," *J. Opt. Soc. Am. A. Opt. Image. Sci. Vis.*, vol. 27, pp. 2106–2114, 2010.

[26] M. R. Pointer, "The gamut of real surface colors," *Color. Res. Appl.*, vol. 5, pp. 145–155, 1980.

[27] R. Zhu, Z. Luo, H. Chen, Y. Dong, and S. T. Wu, "Realizing rec. 2020 color gamut with quantum dot displays," *Opt. Exp.*, vol. 23, pp. 23680–23693, 2015.

[28] O. Masuda and S. M. C. Nascimento, "Lighting spectrum to maximize colorfulness," *Opt. Lett.*, vol. 37, pp. 407–409, 2012.

[29] R. Zhu, G. Tan, J. Yuan, and S. T. Wu, "Functional reflective polarizer for augmented reality and color vision deficiency," *Opt. Exp.*, vol. 24, pp. 5431–5441, 2016.

[30] J. S. Werner, B. Marsh-Armstrong, and K. Knoblauch, "Adaptive changes in color vision from long-term filter usage in anomalous but not normal trichromacy," *Curr. Biol.*, vol. 30, pp. 3011–3015, 2020.